Supporting Information

Strong, Long, Electrically Conductive and Insulated Coaxial Nanocables

Aykut Aydin,[†] Lu Sun,[‡] Xian Gong,[‡] Kasey J. Russell,[§] David J. D. Carter,[§] and Roy G. Gordon[*,†,‡]*

[†]Department of Chemistry and Chemical Biology, Harvard University, Cambridge, Massachusetts, 02138, United States

[‡]John A. Paulson School of Engineering and Applied Sciences, Harvard University, Cambridge, Massachusetts, 02138, United States

[§]The Charles Stark Draper Laboratory, Inc., Cambridge, Massachusetts, 02139, United States

*Corresponding author: gordon@chemistry.harvard.edu

Experimental Details

Technical Details on Electrospinning Optimization

Electrospinning was initiated by applying a +12 kV voltage to the nozzle with respect to the grounded collector. After the jet was initiated, fiber diameter and alignment were optimized by lowering the voltage to as low as 5-6 kV without stopping the jet. Once the voltage was turned on at 12 kV, a droplet at the nozzle typically grew and ejected after a few seconds, to form a continuous jet (Video S2). A rotating drum collector (EM-RDC, IME Technologies) covered with aluminum foil was used to prepare mats of aligned fibers or a rotating spoked-drum collector (EM-RTC with EM-PSD, IME Technologies) with custom windshields was used to prepare single fibers with rotation speeds up to 2500 rpm. (The spoked-drum collector originally comes with 12 spokes, and every other spoke was removed to only have 6 spokes with increased separation.) For making single fibers, the jet was initiated at one end of the collector, and once the jet was stabilized at a selected lower voltage, the nozzle was translated to the other end of the collector (using EM-TNS, IME Technologies) to separate the fibers along the collector. Voltage was manually turned off as soon as the nozzle reached the end of the collector. (If the jet was allowed to continue beyond one pass over the collector, more fibers got deposited that typically crossed and/or stuck to the existing fibers.) A typical experiment lasted under one minute. There was a messy region of fibers around where the jet is initialized on the collector, while the aligned single fibers covered the rest of the collector. The area of the messy fiber region decreased with decreasing nozzle-to-collector separation.

If the solution droplet at the nozzle ages prior to spinning, it starts to dry out and lead to ribbon-shaped fiber formation, even under low-humidity and high-voltage conditions. Ideally, a fresh polymer solution droplet is generated at the nozzle just before starting the jet, but we often need to wait to let the chamber equilibrate before experiments. If this wait is too long, we occasionally obtain ribbons. We rely on visual inspection to remove these ribbons from the workflow. Ribbon shaped fiber morphology correlates with a streaked appearance of the fibers that is visible to the naked eye (Figure S2). Visual inspection can thus be used to spot when ribbons form under such atypical conditions due to the solution droplet becoming dry or cloudy. A bright light source is essential for visual inspection of fibers.

Fiber Handling

We used custom frames of varied dimensions for taking the fibers off the spoked collector and holding them during depositions. The spoke-to-spoke separation was 4.5 cm (after we removed every other spoke to increase this separation, Figure S1-a) on the collector. For getting the highest yield, we placed acrylic frames of matching width on three sides of the collector first (Figure 1-b). Then, narrower frames with double-sided tape along their long edges were brought into contact with the fibers to collect them. Without adding the larger holders that press onto the fibers at their points of contact with the spokes, harvesting fibers from one side of the collector often causes fibers to get pulled from adjacent faces of the 6-sided collector.

It is best to break the fibers away from the frames forcibly during transfer, as merely bringing the holder with tape in contact with the fibers and then pulling away may leave fibers behind; i.e., the strength of the adhesive (for a tape that is often ¼” wide) is often not enough to break the fibers when pulled away.

For PVD, we either added another top frame to the existing double-sided tape, or we added screws on four corners of a frame where we had threaded holes (Figure S1-c). This was done so that the holder can be flipped between two PVD depositions to improve conformality without bringing the fibers in contact with a surface to which they might possibly adhere. Qualitatively, we found that the fibers can be brought into contact and lifted back from smooth Si wafer or glass surfaces, but if they get into contact with a plastic surface, they often

strongly adhere to it and break off the holder. Most of the holders and screw caps we used are 1/8” thick, but we also used 1/16” thick top and bottom frames for certain sputtering experiments that required thinner samples.

We used double-sided Kapton tape (McMaster-Carr, Product Numbers 7361A11 or 7361A12) for most of our deposition experiments. Especially during dry seasons, Kapton tape often becomes non-sticky, in which case we revived its adhesiveness by wetting it with isopropanol before starting to collect fibers. For parts that did not need to go into a deposition chamber (transfer holders, fixing holders to surfaces, etc.), we used a fiber glass reinforced cloth masking tape (McMaster-Carr, Product Number 7577A1) which is more conveniently handled and can be removed from most surfaces without leaving a residue.

Between experiments, we kept the frames in petri dishes that we often stored in a desiccated environment or vacuum sealed in a plastic bag with some silica gel packs. When first placing the fibers into a petri dish, it is important to get rid of static charging by applying an anti-static gun. Both the insides of the bottom and top components of the petri dish need to be thoroughly neutralized; otherwise fibers sag and become slack. Brief tests show this sagging is reversible, but if left sagging, the fibers can slip on the tapes from the sides and sag permanently; this adds a complication to the conformality of a CVD coating. Especially when using wide gapped (Figure S1-c) or thin (1/16”) holders, this sagging can cause the fibers to touch the bottom of the plastic dish, at which point they become strongly attached and eventually break.

For ALD and CVD processes operating at high temperatures, we needed to use a mechanically clamped holder without glue, as discussed in the main text. Our clamped holder design consists of 3.5”x1” frames with a central gap of 0.52” with three holes along the long edges that are threaded for the bottom part and through holes for the top part. More holes increase grasping efficiency at the cost of potentially breaking fibers in their vicinity. We found it necessary to add a layer of Kapton film (typically by attaching it to the bottom frame with double-sided tape on the edges) that serves as a gasket. Without that, we more commonly observe fibers breaking during depositions – especially for the CVD processes that operate at a larger flow rate of gases. Fibers were first transferred onto an acrylic frame with a gap that is larger than the mechanical holder. We used the same acrylic holders with a width matching the spoke separations that we described above for fixing the 6 sides. The bottom part of the clamped holder is fixed on a surface (using large pieces of double-sided tape). The intermediate holder is then placed so the fibers stretch along the bottom part of the holder, and the intermediate tape is also fixed on the same surface. The top frame is then lowered gently onto the bottom part, sandwiching the fibers in the middle (Figure 1-c), and screwed in place. Afterwards, the transfer holder can be removed, breaking fibers outside the clamped region seemingly without affecting the fibers within. If the fibers are held strongly, we can avoid fibers breaking during CVD. Figure 1-d shows a mechanically clamped holder with fibers after being coated with CVD. Apart from serving as a pliable gasket layer, the polymer film might also be enhancing grasping efficiency due to strong van der Waals forces with the fibers. We found that after depositions, if the top frame is gently removed, many fibers often remain suspended and attached to the Kapton film on both sides (though they certainly break in the absence of a Kapton film).

Humidity Dependent Morphology Evolution

After having initial success in controlling the fiber shape, we encountered a second morphological problem when the weather became warmer and more humid: We started observing increased roughness with protrusions or "bumps" on the fibers and their coated wire versions (Figure S3-a). While fibers are highly smooth just after electrospinning (Figure S3-b) when the chamber humidity is kept low, they quickly start forming protrusions when exposed to even mildly humid air at ~30% RH (Figure S3-c). We can roughly simulate longer term exposure to humid air by having a high flow rate of humid air go through a frame of

suspended fibers (for shorter times), and this was done for Figures 3-d and e at relative humidity of 45% and 60%, respectively, which yields substantially porous crystallite growth out of the fibers. Fibers appear to remain smooth under 20% RH and start roughening when standing in air with RH somewhere between 20-25% at 24 °C.

The humidity-dependent formation of rough structures on the fibers is consistent with a mechanism based on deliquescence of $CaCl_2$: when air humidity is above the critical relative humidity of $CaCl_2$, it absorbs water to form a solution that beads up on the fibers (Figure S4). These droplets possibly form the porous protrusions on the fibers when rapidly dried under vacuum during PVD. Slower evaporation under dry air seems to form crystallites shown in Figure S3-d and e, instead. Increased contrast is observed at the protrusions under TEM (Figure S4-b and c), which agrees with stronger electron scattering from heavier Ca and Cl atoms compared to PMIA. Cross-sections at the bumps reveal a darker core region with the same contrast as that of the core of smooth parts of the coated fibers, likely being that of PMIA, along with a porous brighter region around this core, likely being that of $CaCl_2$ (Figure S4-d and e).

We investigated various treatments for removing the $CaCl_2$ present in the fibers. Directly exposing suspended fibers on a frame to a stream of water or trying to dip and remove them from a container of water often breaks some of the fibers due to capillary forces as the fibers pass the water-air interface. We tried lowering the surface tension of water with surfactants or various alcohols with lower surface tension, but the fibers still broke. One strategy that works is to support fibers temporarily with a smooth surface (such as a Si wafer) during direct washing, and then to remove the support. We also tried exposing fibers to a mist of steam such that water droplets collect on the fibers and run down, washing away the salt. Hanging the fibers above a beaker full of hot, steaming water seems to induce very large agglomerations of $CaCl_2$ along the fibers (Figure S3-f) as the droplets do not run down efficiently. Suspending a frame of fibers in front of a mist stream of water droplets generated from a sonicating humidifier does induce effective washing by movement of droplets along the fibers (Figure S5 and Video S3). This leads to relatively smooth fibers (Figure 3-g). We further exposed fibers washed with such a humidifier to a high flow rate of 60% RH air (akin to the conditions in Figure 3-e) and observed much less roughening as shown in Figure 3-h, which suggests that most of the salt is removed with the mist-based washing treatment. To keep wires from roughening in general, the fibers were not washed, but simply kept in dry storage conditions (e.g., stored in vacuum, under nitrogen, or in dry air with silica gel packs).

Supporting Figures

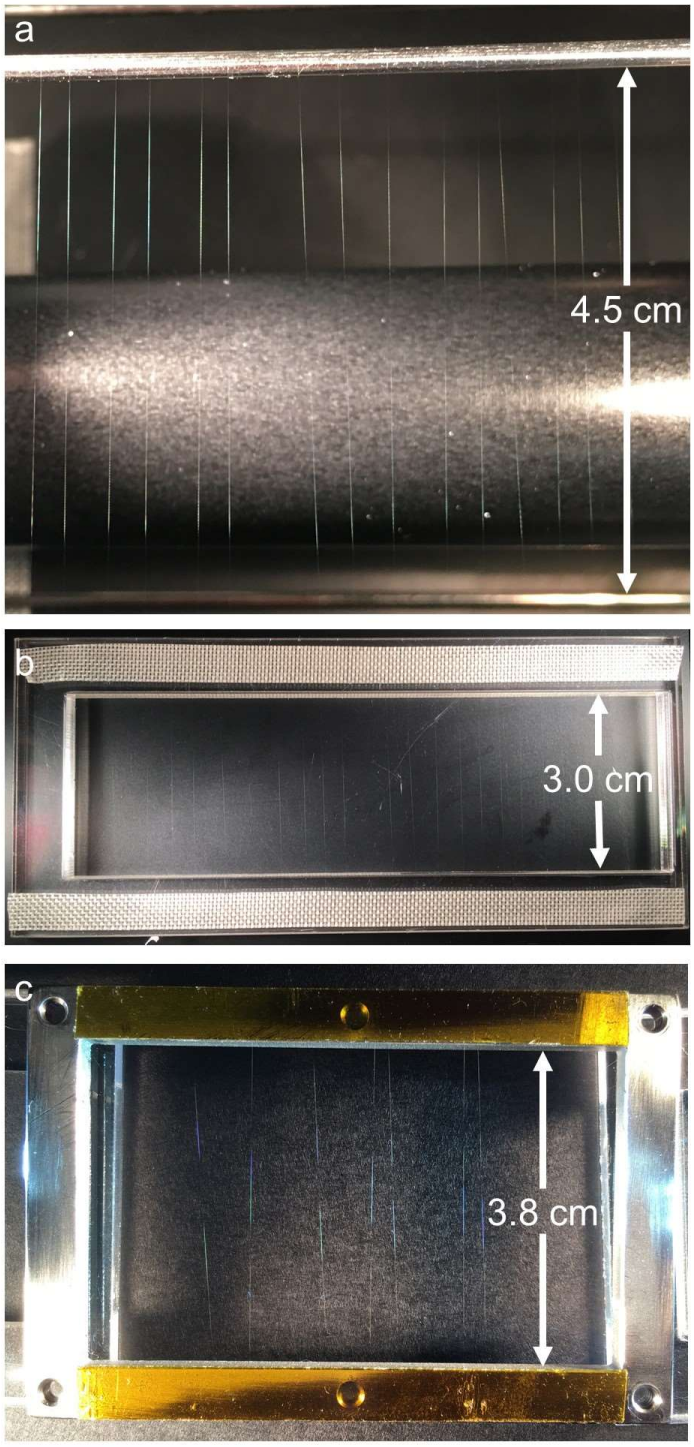

Figure S1. Photographs of fibers. (a) Photograph of aligned fibers on part of the rotating spoked-drum collector. (b) Photograph of aligned fibers on a transfer holder. (c) Photograph of our widest holder with some single fibers attached by double-sided tape that is suitable for PVD. Bright illumination from the side results in scattered light from the submicron fibers, making them visible to the naked eye.

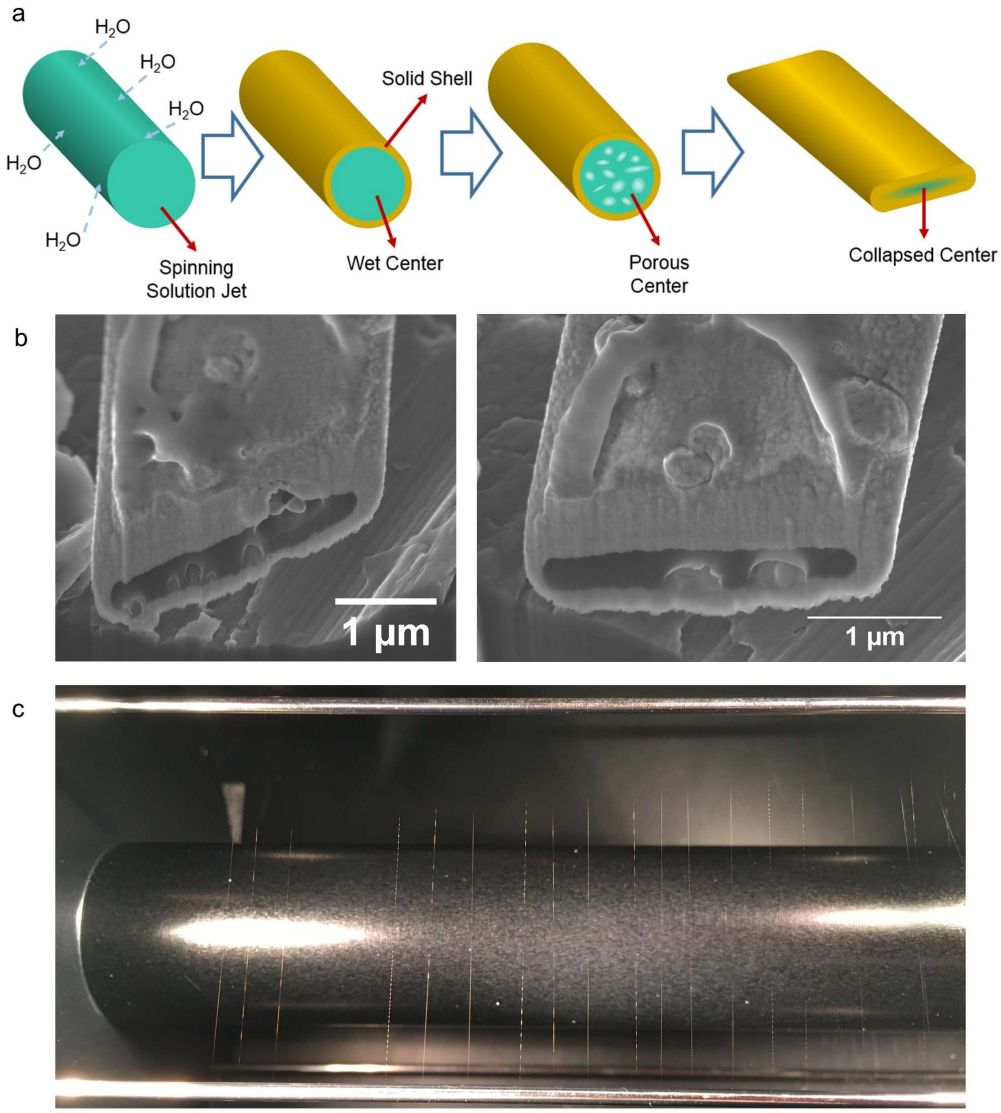

Figure S2. Ribbon shaped fiber formation and visual appearance: (a) Ribbon Shaped Fiber Formation Hypothesis: Water diffuses into the spinning jet, causing precipitation of the polymer on the periphery. Solidified shell fixes the outer diameter of the structure, and the still liquid solution within evaporates over time, leaving behind a porous structure. This porous structure gets crushed by ambient pressure to form the ribbon shape. (b) Some pores do not get crushed and are visible in the fiber cross sections. (c) Visual appearance of dashed lines that correlate with ribbon shaped fibers.

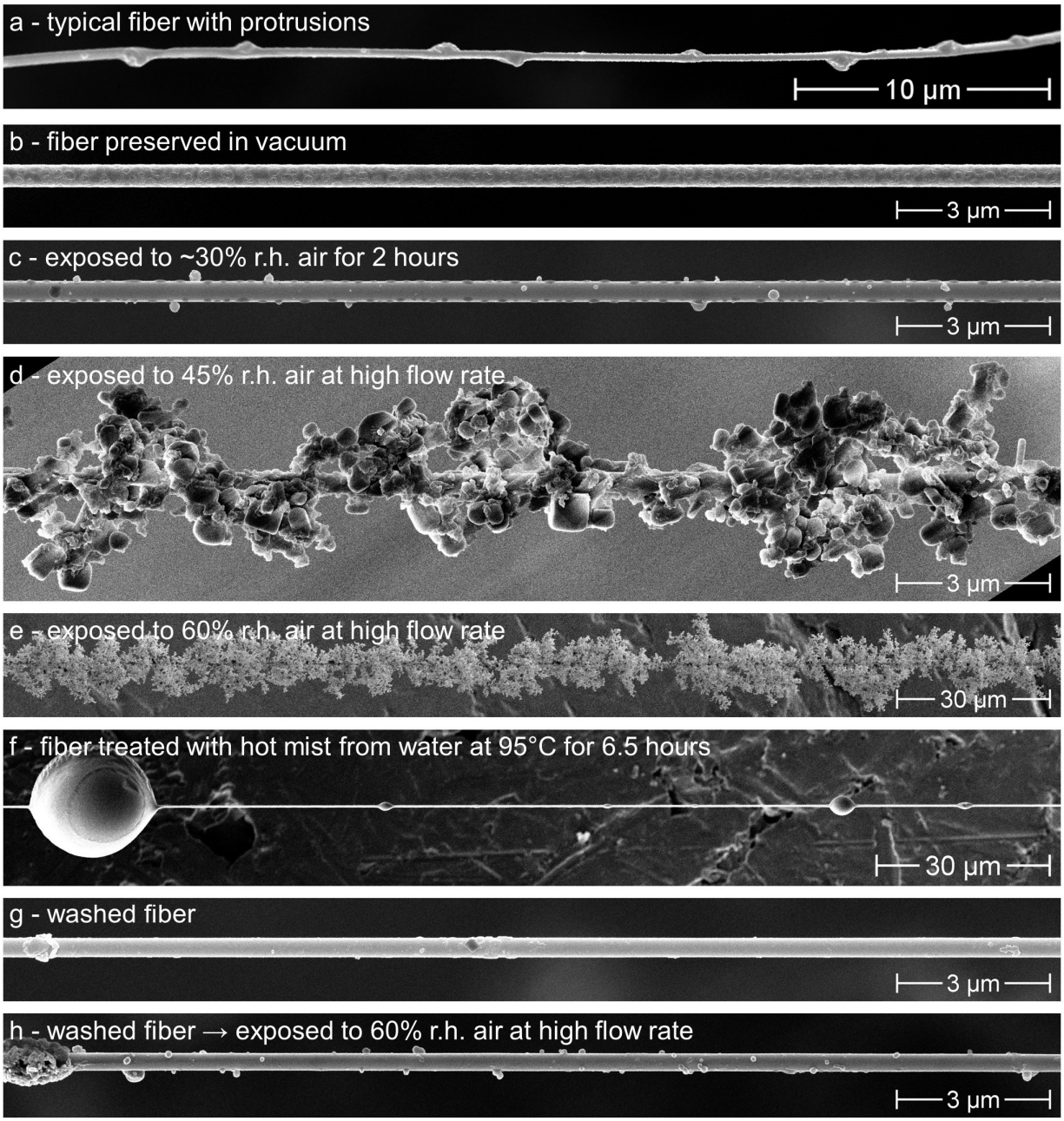

Figure S3. Humidity-dependent morphology evolution: (a) SEM image of a bumpy Pt/Pd alloy (80/20) coated PMIA fiber. (b) Fiber kept in vacuum for 2 hours before imaging. (c) Fiber exposed to ambient air at ~30% RH for 2 hours. (d) Fiber annealed with a high flow rate 45% RH air at room temperature. (e) Fiber annealed with a high flow rate 60% RH air at room temperature. (f) Fiber annealed over a beaker of hot water for 6.5 hours. (g) Fiber where $CaCl_2$ is mostly removed by treatment with an ultrasonic humidifier for 6 hours. (h) After $CaCl_2$ was removed with the previous treatment, fibers were exposed to a high flow rate of 60% RH air as in part d, but they did not roughen nearly as much. (All fibers were coated with a thin layer of Pt/Pd alloy (80/20) to assist with imaging.)

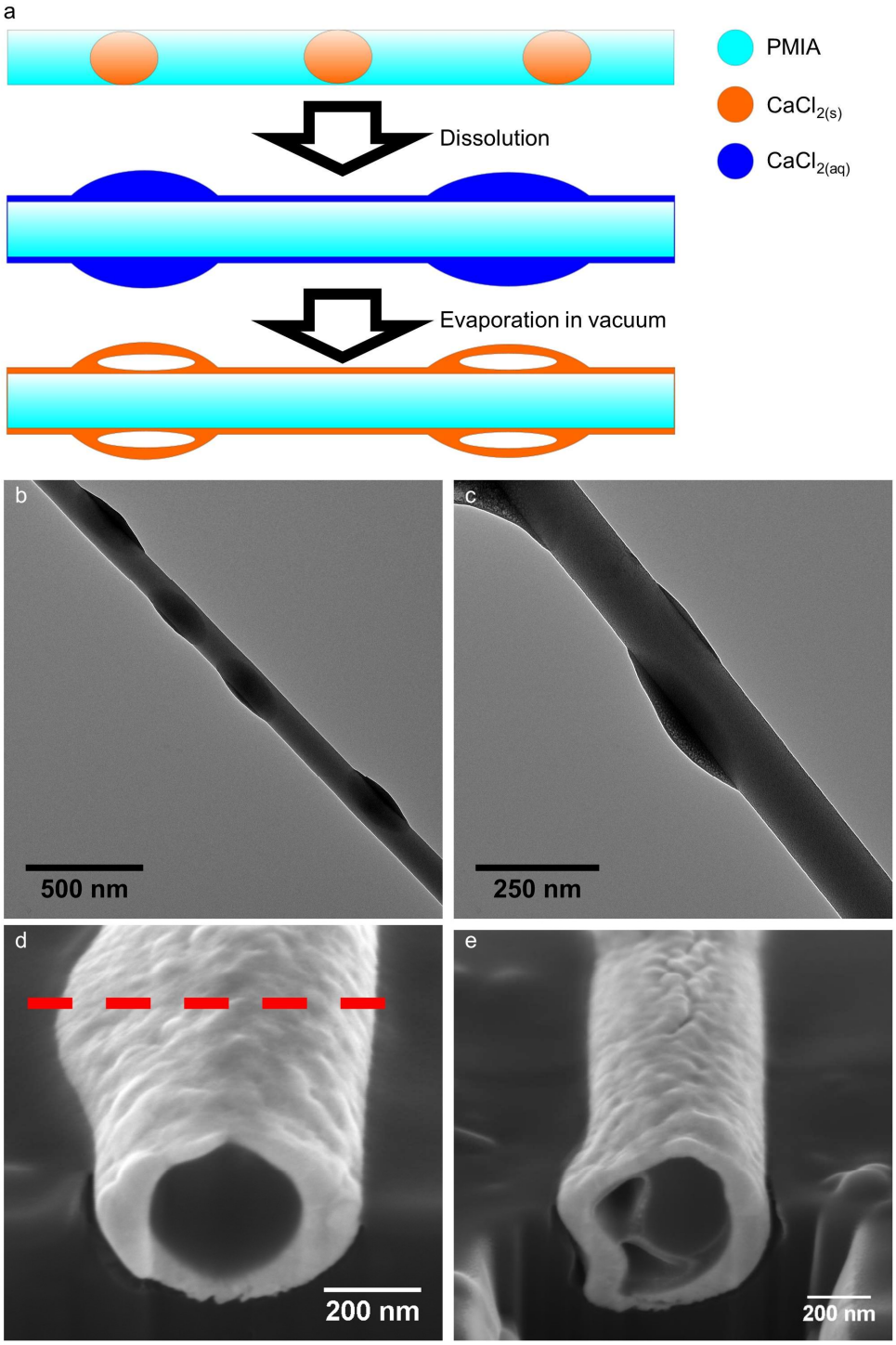

Figure S4. Morphology evolution mechanism: (a) Proposed mechanism for the formation of the protrusions: $CaCl_2$ dissolves upon capturing air humidity, forming droplets along the fibers. The droplets rapidly dry under vacuum to form porous beads. (b and c) TEM images of PMIA fibers with protrusions. The protrusions appear darker, consistent with the higher atomic mass of $CaCl_2$. (d) Cross section of a metal coated PMIA fiber at a round part. Also indicated with the red line is where the next cross section in part (e) was performed. (e) Cross section of the same fiber at a protrusion. The fiber core has different contrast than the porous structure.

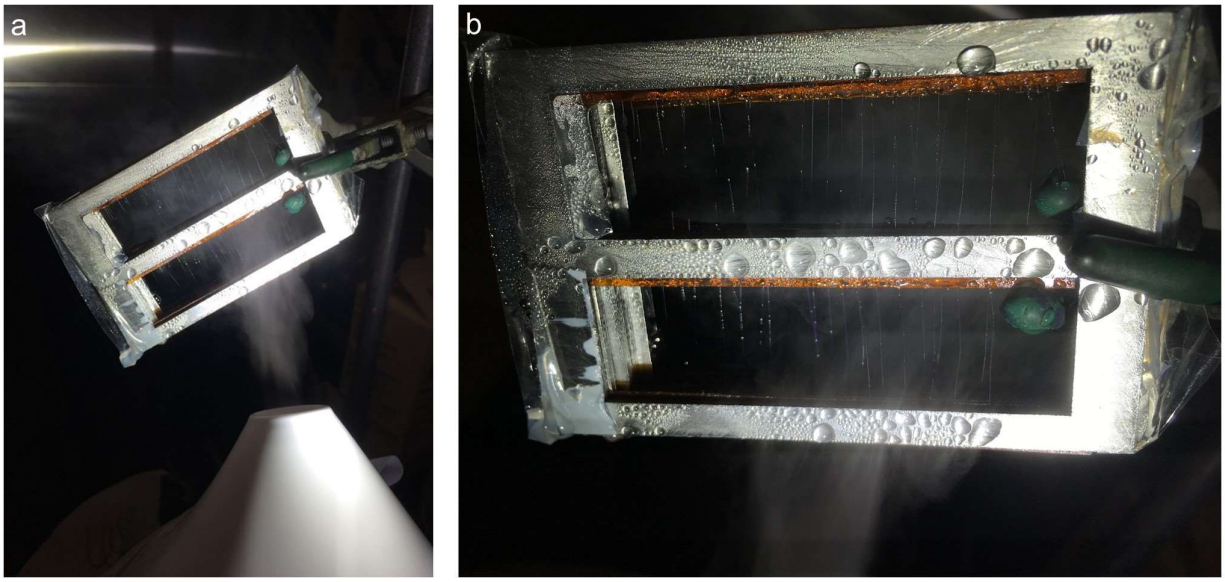

Figure S5. Water mist-based nanofiber washing for removing $CaCl_2$: (a-b) Photographs of a stack of three holders with nanofibers being exposed to water mist from a sonicating humidifier. Small droplets accumulating on the fibers can be seen. (See also: Video S3.)

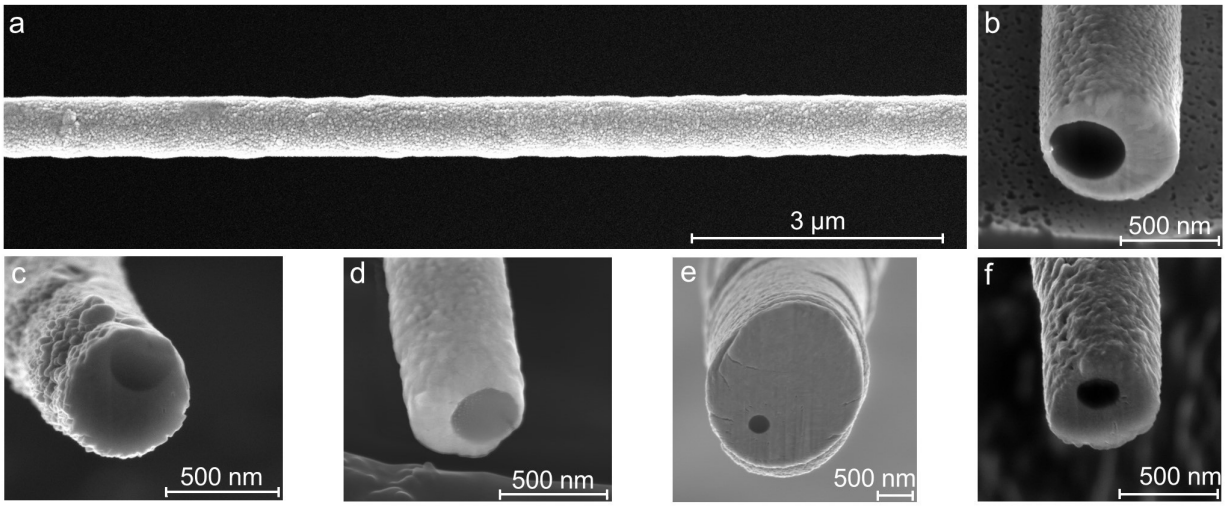

Figure S6. (a) Platinum sputter coated fiber and (b) its cross-section. (c) Cross-section of a fiber sputter coated with titanium from one side only. Cross-sections of (d) gold, (e) copper, and (f) cobalt coated fibers sputtered from both sides.

List of Supplementary Videos

- **Video S1.** Yarning fibers during electrospinning.
- **Video S2.** Typical PMIA electrospinning experiment.
- **Video S3.** Water mist-based fiber washing.